3.2. MODEL REFERENCE ADAPTIVE CONTROL OF PERMANENT MAGNET SYNCHRONOUS MOTOR DRIVE WITH FORCED DYNAMICS

***Abstract*:** A speed control system for electrical drives employing synchronous motors (SM) is presented offering high robustness to parameter uncertainties and external load torques. A triple-loop cascade control structure is employed in which the inner loop is a stator current control loop and the middle loop is a shaft sensorless speed control loop, which is based on the forced dynamic control principle. Forced dynamic control, as well as converting the non-linear SM into a linear element, alone offers generally higher robustness than conventional shaft sensorless vector control methods, through using a time-varying load torque estimate. This robustness is further improved here by adding an outer loop based on the model reference adaptive control (MRAC) principle, which is an alternative technique to the sliding mode control outer loop presented in section 2.3. Any of the forced dynamic modes presented in Chapter 1 can be used and results are presented here for the *constant acceleration*, *linear first order* and *linear second order* modes. For simplicity, the outer MRAC control loop is introduced with the middle loop operating in the linear first order mode, which yields a first order closed-loop system whose pole location can be chosen by the user. Also, in this mode (and any other linear mode) the drive may be included as an actuator in a larger scale control scheme to which linear control system design methods can be applied. Experimental results presented show good correspondence with theoretical predictions.

3.2.1 Introduction

The addition of an outer loop employing a robust control technique, in this case MRAC, to improve robustness is applicable in many control applications and it should be noted that it may be used for induction motor drives as well as SM drives. It is necessary, however, for the basic control system around which the robust outer loop is closed to yield dynamics of known order (first order in the case under study). In view of its importance, the basic control system development is completely described below, prior to introduction of the robust outer loop, and this entails some repetition of material presented in previous sections.

In recent years „*sensorless*“ or „*self-sensing*“ control of AC machines has been extensively researched. The cost and reliability advantages, when mechanical sensors and connection cables are eliminated for the measurement of position or velocity to close a feed-back loop, have been the driving force behind this research activity.

The basic drive system without the outer loop is based on the new control method of electric drives employing SM introduced in section 3.1.2. Forced dynamic control yielding the first order linear dynamic mode is a form of feedback linearisation [1] and it is made possible by employing an inner current control loop and an observer for rotor speed estimation based on the sliding mode control principle [2]. This approach was introduced in [3] and [4]. The system operates without shaft sensors, only the stator currents being measured, the applied stator voltages being determined by the computed inverter switching algorithm and with a knowledge of the DC link voltage. The prescribed response to the reference speed has linear first order dynamics, together with the vector control condition of mutual orthogonality between the stator current and rotor flux vectors (assuming perfect estimates of the motor parameters). The original basic SM drive control system with forced dynamic control which contains, in addition, a set of two observers for estimation of the rotor speed and the load torque using the magnetic flux components from a flux estimation algorithm was shown in Fig. 3.1.1.

Forced dynamic control is applicable in many non-linear multivariable automatic control applications and originally was developed for electrical drives with induction motors and later applied also for electric drives with SM [5]. The drive presented here would be very convenient also as an inner speed control loop for a position servo-system.

Since the control law itself, the magnetic flux calculator, the rotor speed observer and load torque observer are all model-based, i.e., dependent on estimates of the motor parameters, then some sensitivity to the errors in these estimates would be expected. This means that the closed-loop performance of the whole control system will be affected, to some extent, by errors in the aforementioned estimates. The intention here is to reduce this sensitivity by closing a simple model referenced adaptive control loop around the original close-loop system and to improve the robustness of the whole control system. This results is the overall control block diagram shown in Fig. 3.2.1.

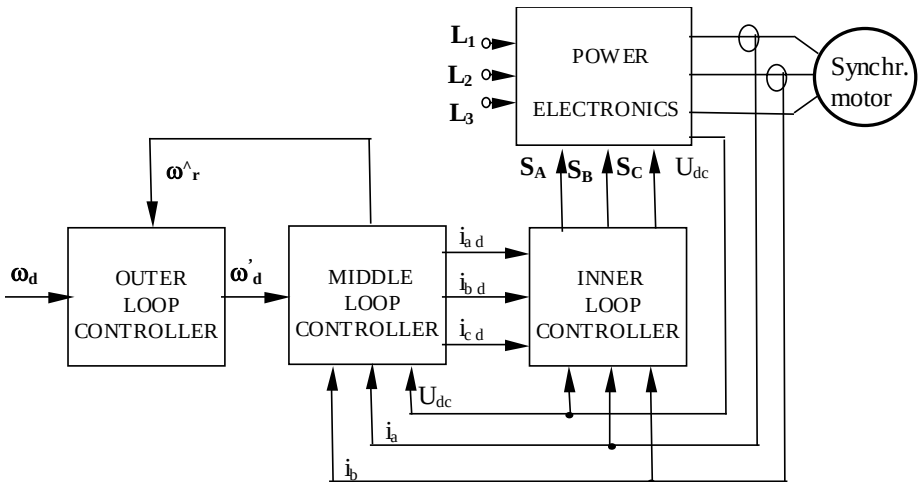

Fig. 3.2.1 Modified block diagram of the overall control system with MRAC

3.2.2 Control System

2a) The middle loop controller

The forced dynamic control law is embodied in the middle loop controller. This control law forces the SM rotor speed estimate, $\hat{\omega}_r$, to follow the corresponding demand, ω'_r, from the outer loop controller with a linear, first order dynamic lag having a chosen time constant of T_ω. This in turn, causes the real SM rotor speed, ω_r, to be controlled to an accuracy dependent on the closeness with which the estimate, $\hat{\omega}_r$, follows real ω_r. This controller also contains rotor speed and load torque estimation algorithms using the measured stator currents, i_a, i_b, and i_c, together with the measured voltage of the DC supply and the computed stator voltages, u_a, u_b, and u_c, from inverter switching algorithm.

2b) Model of Motor and Load

The permanent magnet SM model in the rotating d, q co-ordinate system is used:

$$\frac{d}{dt}\begin{bmatrix} i_d \\ i_q \end{bmatrix} = \begin{bmatrix} \frac{-R_s}{L_d} & p\omega_r \frac{L_q}{L_d} \\ -p\omega_r \frac{L_d}{L_q} & \frac{-R_s}{L_q} \end{bmatrix} \cdot \begin{bmatrix} i_d \\ i_q \end{bmatrix} - \frac{p\omega_r}{L_q}\begin{bmatrix} 0 \\ \Psi_{PM} \end{bmatrix} + \begin{bmatrix} \frac{1}{L_d} & 0 \\ 0 & \frac{1}{L_q} \end{bmatrix} \cdot \begin{bmatrix} u_d \\ u_q \end{bmatrix} \qquad (3.2.1)$$

(3.2.2)

$$\frac{d\omega_r}{dt} = \frac{1}{J}\left\{c_5\left[\Psi_{PM} i_q + \left(L_d - L_q\right) i_d i_q\right] - \Gamma_L\right\} = \frac{1}{J}\left\{\Gamma_{el} - \Gamma_L\right\}, \qquad (3.2.3)$$

where i_d, i_q and u_d, u_q are, respectively, the stator current and voltage components, ω_r is the rotor angular velocity and Γ_L is the external load torque. Three-phase SM Andover 4ANTS SP 10 5AB parameters are as follows: P_n = 400 W at n_n = 3000 rpm, 2p = 6; R_S = 36,5 Ω, L_d = 50 mH, L_q = 50 mH, Ψ_{PM} = 0,312 Wb and the lumped moment of inertia is J = 0,003 kgm^2.

2c) Master control law

This is based on *linearising functions* [1], which force a non-linear system to obey specified linear closed-loop differential equations:

$$\frac{d\omega_r}{dt}=\frac{1}{T_\omega}\left(\omega_d-\omega_r\right). \tag{3.2.4}$$

Equation (3.2.3) for the rotor angular velocity is made to follow equation (3.2.4) by equating the right hand sides:

$$\frac{1}{J}\left\{c_5\left[\psi_d i_q-\psi_q i_d\right]-\Gamma_L\right\}=\frac{1}{T_\omega}\left(\omega_d-\omega_r\right) \tag{3.2.5}$$

The rotor magnetic flux calculator estimates the individual magnetic flux components, Ψ_d and Ψ_q, for the control algorithm:

$$\begin{aligned}\psi_d^*&=\tilde{L}_d i_d+\tilde{\Psi}_{PM}\\ \psi_q^*&=\tilde{L}_q i_q\end{aligned} \tag{3.2.6}$$

The second part of the control law is formulated on the basis of the PMSM construction, when maximum torque sensitivity is achieved with:

$$i_d = 0\ . \tag{3.2.7}$$

Taking into account equation (3.2.7) the required i_q can be found from (3.2.5). These two current components are then used to generate the *demanded* values of i_d and i_q which are denoted as i_{d_d} and i_{q_d}. In the implemented control law the previously defined state variables and motor parameters have to be replaced by their estimates:

$$i_{d\_d}=0 \tag{3.2.8}$$

$$i_{q\_d}=\frac{1}{c_5\tilde{\psi}_{PM}}\left[\hat{\Gamma}_L+\frac{\tilde{J}}{T_\omega}\left(\omega_d-\hat{\omega}_r\right)\right]=\frac{1}{c_5\tilde{\psi}_{PM}}\left[\hat{\Gamma}_L+\tilde{J}\cdot a_d\right]. \tag{3.2.9}$$

This is the basic master control law, which may be used for all the operational modes. As mentioned previously, this requires a load torque estimate and a means of obtaining this is presented in the following section.

2d) State Estimation and Filtering

2d1) The pseudo sliding mode observer and angular velocity extractor

Modified version of the stator current vector pseudo sliding-mode observer is based on equations (3.2.1) and (3.2.2) as a real time model but *purposely using only the terms without* ω_r, these being replaced by the model correction inputs, $v_{eq\,d}$ and $v_{eq\,q}$. Thus:

$$\frac{d}{dt}\begin{bmatrix} i_d^* \\ i_q^* \end{bmatrix} = -\begin{bmatrix} \frac{R_s}{L_d} & 0 \\ 0 & \frac{R_s}{L_q} \end{bmatrix} \cdot \begin{bmatrix} i_d^* \\ i_q^* \end{bmatrix} + \begin{bmatrix} \frac{1}{\tilde{L}_d} & 0 \\ p & \frac{1}{\tilde{L}_q} \end{bmatrix} \cdot \begin{bmatrix} u_d \\ u_q \end{bmatrix} + \begin{bmatrix} v_{eq\,d} \\ v_{eq\,q} \end{bmatrix} \tag{3.2.10}$$

where i^*_d and i^*_q are estimates of i_d and i_q as in a conventional observer. In a classical sliding-mode observer, the useful outputs are the continuous *equivalent values* of the rapidly switching variables:

$$\begin{bmatrix} v'_{eq\,d} \\ v'_{eq\,q} \end{bmatrix} = V_{max}\,\mathrm{sgn}\begin{bmatrix} i_d - i_d^* \\ i_q - i_q^* \end{bmatrix}. \tag{3.2.11}$$

This, however, does not directly generate $v_{eq\,d}$ and $v_{eq\,q}$. To achieve this, a *pseudo-sliding-mode* observer [4] may be formed by replacing equation (3.2.11) with:

$$\begin{bmatrix} v_{eq\,d} \\ v_{eq\,q} \end{bmatrix} = K_{sm}\begin{bmatrix} i_d - i_d^* \\ i_q - i_q^* \end{bmatrix}, \tag{3.2.12}$$

where the gain, K_{sm}, is made as high as possible within the stability limit set by the sampling time of the digital implementation. For large K_{sm}, the errors between the real currents and the estimated currents from the observer are driven almost to zero, resulting in (3.2.13):

$$\begin{bmatrix} v_{eq\,d} \\ v_{eq\,q} \end{bmatrix} = \begin{bmatrix} 0 & p\omega^*_r \frac{\tilde{L}_q}{\tilde{L}_d} \\ -p\omega^*_r \frac{\tilde{L}_d}{\tilde{L}_q} & 0 \end{bmatrix} \cdot \begin{bmatrix} i_d \\ i_q \end{bmatrix} - \frac{p\omega^*_r}{\tilde{L}_q}\begin{bmatrix} 0 \\ \tilde{\Psi}_{PM} \end{bmatrix} \tag{3.2.13}$$

and this may be manipulated to yield an unfiltered rotor speed estimate, ω^*_r. Thus:

$$\omega_r^* = \frac{-\tilde{L}_q v_{eq\,q}}{p\cdot\left(\tilde{L}_d i_d + \tilde{\Psi}_{PM}\right)}. \qquad (3.2.14)$$

2d2) Observer for Load Torque Estimation and Rotor Speed Estimate Filtering

The load torque estimate required by the master control law is provided here by a standard observer having a similar structure to a Kalman filter, a direct measurement of this variable being assumed to be unavailable. The real time model of this observer is based on the motor torque equation (3.2.3). The observer correction loop is actuated by the error between the rotor speed estimate, ω^*_r, from the angular velocity extractor of the previous section and the estimate, $\hat{\omega}_r$, from the real time model. The observer equations are:

$$\begin{aligned} e_\omega &= \omega_r^* - \hat{\omega}_r \\ \dot{\hat{\omega}}_r &= \frac{1}{\tilde{J}}\left[\tilde{c}_5\left(\Psi_d^* i_q - \Psi_q^* i_d\right) - \hat{\Gamma}_L\right] + k_\omega e_\omega \\ \dot{\hat{\Gamma}}_L &= k_\Gamma e_\omega \end{aligned} \qquad (3.2.15)$$

Since $\hat{\omega}_r$ is a filtered version of ω^*_r it is used directly in the middle and outer loop controllers. This is a conventional second order linear observer with a correction loop characteristic polynomial, which may be chosen via the gains, k_ω and k_Γ, to yield the desired balance of filtering between the noise from the measurements of i_d and i_q and the noise from the angular velocity measurement, ω^*_r.

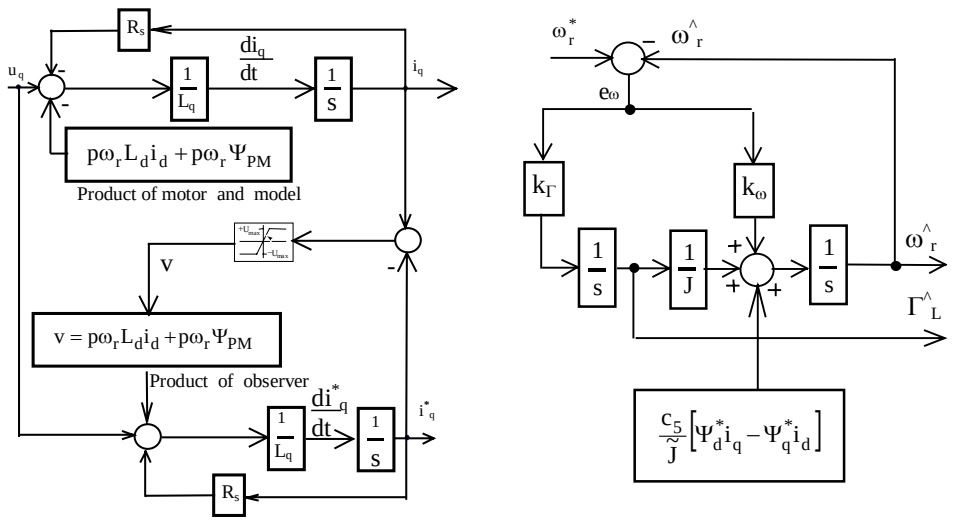

a) Pseudo-sliding mode observer *b) Filtering observer*

Fig. 3.2.2 Modified block diagrams of pseudo-sliding mode and filtering observer

3.2.3 Outer Loop Controller

Since, as stated previously, the middle loop controller is model based, i.e., it contains algorithms depending on estimates of the motor and load parameters, the closed-loop performance will be affected by errors in these estimates. In particular, errors in the estimate of the external load torque, Γ_L, will affect the closed-loop performance. Let the errors introduced by the motor parameter uncertainties, load torque estimate and imperfect operation of the middle control loop due to the non-zero iteration interval be (roughly) represented by a change of time constant and DC gain. Then the real system, formed by the inner and middle control loops can be represented by the following transfer function:

$$\frac{\hat{\omega}_r(s)}{\omega_d'(s)} = \frac{K_d}{1+sT_\omega'} . \tag{3.2.16}$$

The purpose of the outer loop controller is to improve the robustness of the overall control system against uncertain parameters and load torque estimation errors. The outer control loop controller is MRAC based. The model is simply the *nominal* transfer function that would be yielded by the inner and middle loop in perfect operation:

$$\frac{\hat{\omega}_r(s)}{\omega_d'(s)} = \frac{1}{1+sT_\omega} . \tag{3.2.17}$$

Figure 3.2.3 shows the outer model reference control loop using this model.

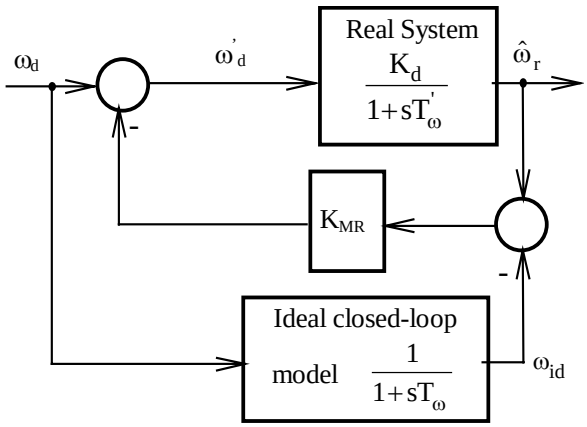

Fig. 3.2.3 Model reference based control loop

The demanded rotor speed, ω'_d, is applied to the basic real system formed by the inner and middle control loops. Any mismatch between the real system and the closed-loop reference model then gives rise to a correction, $K_{MR}\cdot(\hat{\omega}_r - \omega_{id})$, applied to the real system to force it to follow the model. As the model reference control loop gain, K_{MR}, is increased, then, in theory, the error, $\hat{\omega}_r - \omega_{id}$, is reduced, thereby causing the real system to be 'slaved' to the model. Applying Mason's formula to Fig. 3.2.3 yields (3.2.18):

$$\frac{\hat{\omega}_r(s)}{\omega_d(s)} = \frac{\dfrac{K_d}{1+sT'_\omega}\left(1+K_{mr}\dfrac{1}{1+sT_\omega}\right)}{1+\left(K_{mr}\dfrac{K_d}{1+sT'_\omega}\right)}. \qquad (3.2.18)$$

Thus, as K_{MR}, tends to infinity, the transfer function between the estimated speed and the demanded speed tends to the demanded transfer function (3.2.19), predicting the required robustness:

$$\frac{\hat{\omega}_r(s)}{\omega_d(s)} \to \frac{1}{1+sT_\omega} \quad \text{for} \quad K_{mr}\to\infty \qquad (3.2.19)$$

In practice, however, any un-modelled plant dynamics and the non-zero sampling time of the digital processor will limit K_{mr}. A shortfall in robustness would still be expected since this shaft sensorless system depends on the accuracy of the speed estimate, $\hat{\omega}_r$.

3.2.4 Experimental Results

The control algorithms were implemented on a Pentium PC. The stator currents were measured through LEM transformers and evaluated using a PC Lab Card PL818 built into the PC. A six-transistor IGBT module was used as the three-phase inverter. All the experiments presented were carried out with a DC supply voltage of U_{dc} = 90 V and step rotor speed demands of ω_d = 700 RPM and ω_d = 125 rad/s and a time constants of T_ω = 0,5 s and T_ω= 0,2 s. Data logging of the experimental variables was carried out for a 1,75 s and 2 s time interval. The SM was idle running during all the experiments.

In all the graphs presented, the stator current components as functions of time and their complex plot are shown in subplots (a) and (b) during the starting interval t∈(0-0,5 s). The magnetic flux as a complex plot is shown in (c) and its components as functions of time are shown in (d) for the same starting time interval. Plot (e) shows the speed estimate, $\hat{\omega}_r$, from the filtering observer together with the ideal speed response ω_{id}. Finally, subplot (f) shows the ideal rotor speed, ω_{id}, together with real rotor speed , ω_r.

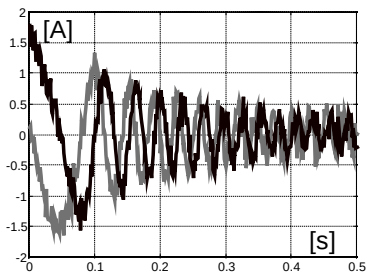

a) stator currents

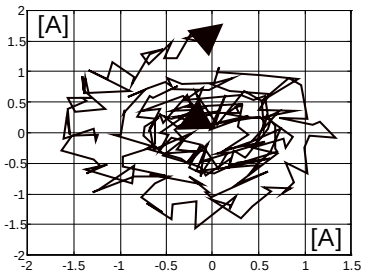

b) complex currents

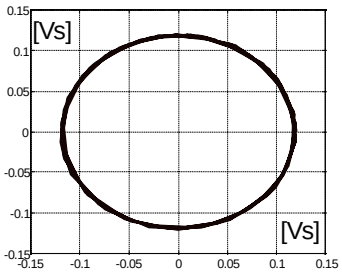

c) complex linkage flux

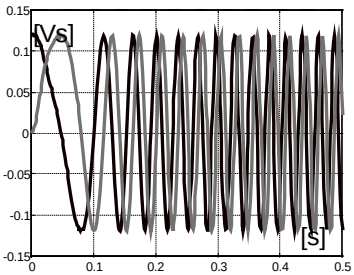

d) linkage mg. flux

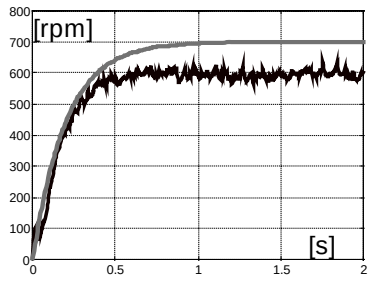

e) ideal & estimated speed

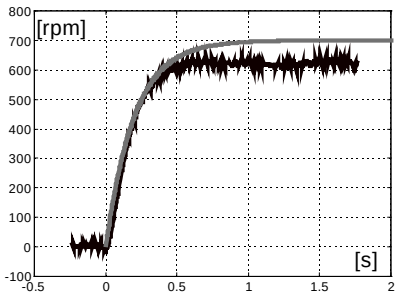

f) ideal & real rotor speed

Fig. 3.2.4 Stator currents, linkage magnetic flux and speed response for first order linear dynamic mode without outer MRAC control loop

The experimental results obtained with the middle and inner control loops, excluding the MRAC loop, are shown in Fig. 3.2.4. The errors between the ideal rotor speed computed according to transfer function (3.2.17) and the estimated and real rotor speeds are visible in subplots (e) and (f) and these errors may be seen to persist even in the steady-state.

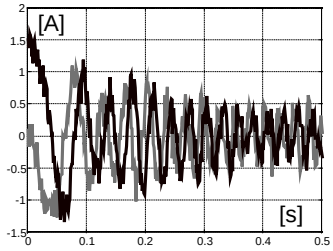

a) stator currents

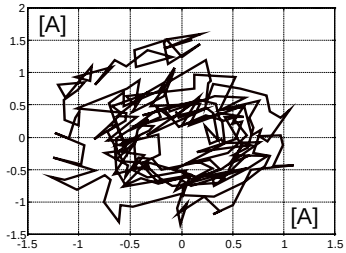

b) complex currents

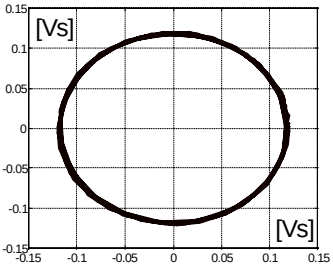

c) complex linkage flux

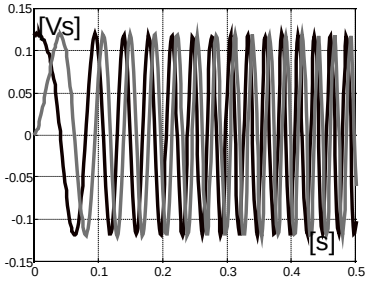

d) linkage mg. flux

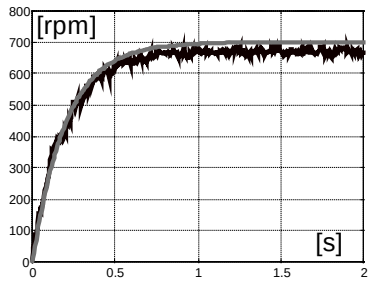

e) ideal & estimated speed

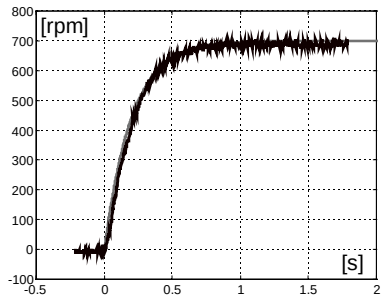

f) ideal & real rotor speed

Fig. 3.2.5 Stator currents, linkage magnetic flux and speed response for first order linear dynamic mode with outer MRAC control loop

Experimental results corresponding to those of Fig. 3.2.4, but including the MRAC outer loop, are shown in Fig. 3.2.5. The significant reduction of the errors between the ideal speed and real rotor speed brought about by the MRAC outer loop, both during the acceleration of the drive and in the steady state, is evident by comparison of these two figures.

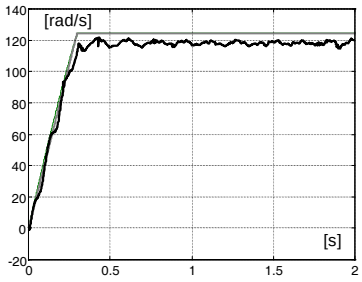

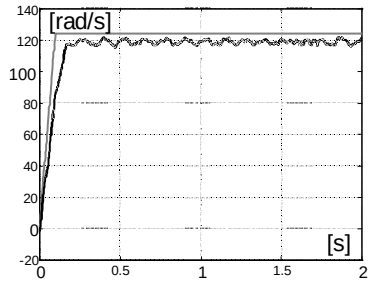

a) constant acceleration

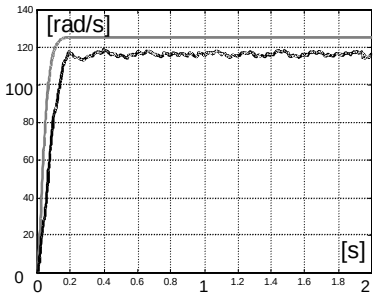

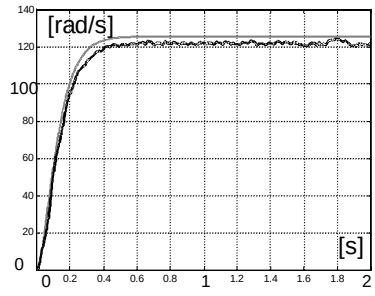

b) linear 1st order dynamic

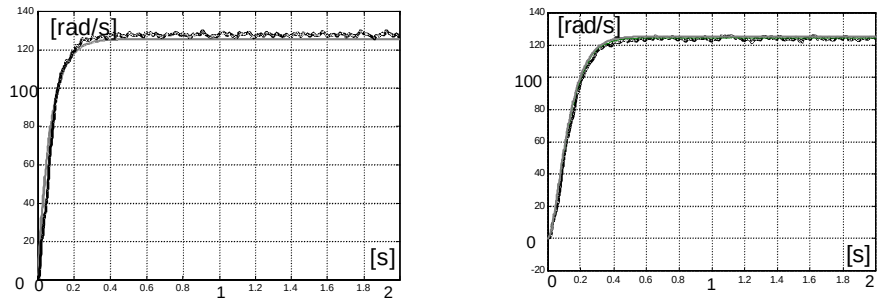

c) linear 2nd order dynamic

Fig. 3.2.6 Speed responses for three dynamic modes without (left graphs) and with (right graphs) outer MRAC control loop

Fig. 3.2.6 shows a comparison of results obtained with and without the MRAC outer loop for the constant acceleration mode and the linear second order mode as well as the linear first order mode. For the two additional dynamic modes, the ideal real-time model of Fig. 3.2.3 must be replaced by that of the appropriate dynamic mode, the equations for which are given in Chapter 1. The significant reduction of the aforementioned errors brought about by the MRAC outer control loop both during the acceleration interval and in the steady-state for all three dynamic modes is evident by comparison of the left and right sides of Fig. 3.2.6.

3.2.5 Conclusions and Recommendations

The preliminary experimental results (for an unloaded permanent magnet SM) confirm that the addition of an MRAC outer control loop to the forced dynamic shaft sensorless speed control system considerably improves its performance. The MRAC loop also rendered the starting position less critical.

Suggestions for future research work are:

a) an investigation of robustness with respect to motor and load parameter uncertainties for both MRAC and SMC outer control loops, including the

addition of an unmodelled mechanical load with referred moment of inertia several times greater than that of the rotor.

b) a further set of experimental trials, including application of step load torques, together with an extensive investigation of the variation of the filtering observer performance with the pole locations.

c) an extensive examination of the starting characteristics of the control system, with respect to the lack of knowledge of the initial rotor position and further work, if necessary, to ensure reliable start-up from any initial rotor position.

3.2.6 References

[1] ISIDORI, A.: '*Nonlinear Control Systems*'. 2nd edition, ***Springer-Verlag*** Berlin, 1990.

[2] UTKIN, V. I.: '*Sliding Modes in Control and Optimisation*'. ***Springer Verlag*** Berlin, 1992

[3] DODDS, S. J, UTKIN, V. A., VITTEK, J.: '*Self Oscillating, Synchronous Motor Drive Control System with Prescribed Closed-Loop Speed Dynamics*'. ***2nd EPE Chapter Symposium*** on 'Electric Drive Design and Applications', Nancy, France, June 1996, pp. 23 - 28.

[4] DODDS, S. J., VITTEK, J.: '*Synchronous Motor Drive with Prescribed Closed-loop Speed Dynamics Employing a Two-phase Oscillator*'. Proceedings of ***EDPE'96***, High Tatras, Slovakia, September 1996, pp. 209 - 216.

[5] DODDS, S. J., VITTEK, J., SEMAN, S.: '*Implementation of a Sensorless Synchronous Motor Drive Control System with Prescribed Closed-Loop Speed Dynamics*'. Proceedings of ***SPEEDAM'98***, Sorrento, Italy, June 1998, pp. P4-5 - P4-10.

[6] VITTEK, J., ALTUS, J., DODDS S. J., PERRYMAN, R.: '*Preliminary Experimental Results for Synchronous Motor Drive with Forced Dynamics*'. Proceedings of ***IASTED CA'98*** Conference on '*Control and Applications'*, August 1998 Honolulu, HI, USA, pp. 219 - 223.

[7] VITTEK, J., ALTUS, J., BUDAY, J., MIKLO, J.: *'MRAC Improves Performance of Induction Motor Drive with Forced Dynamics'*. Proceedings of ***IASTED ICS'99*** International Conference on '*Intelligent Control and Systems*', Oct. 1999, Santa Barbara, CA, USA, pp. 85 – 90.

Acknowledgements

The authors wish to thank the **European Commission, Brussels**, for funding the **INCO Copernicus** programme No.960169 **UCODRIVE.**